We are IntechOpen, the world's leading publisher of Open Access books Built by scientists, for scientists

4,800
Open access books available

122,000
International authors and editors

135M
Downloads

Our authors are among the

154
Countries delivered to

TOP 1%
most cited scientists

12.2%
Contributors from top 500 universities

WEB OF SCIENCE™

Selection of our books indexed in the Book Citation Index in Web of Science™ Core Collection (BKCI)

Interested in publishing with us?
Contact book.department@intechopen.com

Numbers displayed above are based on latest data collected.
For more information visit www.intechopen.com

10

Phosphorescence Oxygen Analyzer as a Measuring Tool for Cellular Bioenergetics

Fatma Al-Jasmi, Ahmed R. Al Suwaidi, Mariam Al-Shamsi, Farida Marzouqi, Aysha Al Mansouri, Sami Shaban, Harvey S. Penefsky and Abdul-Kader Souid
United Arab Emirates University, Faculty of Medicine and Health Sciences
Abu Dhabi
United Arab Emirates

1. Introduction

The "*phosphorescence oxygen analyzer*" and its use to monitor O_2 consumption by cells and tissues are discussed in this chapter (Lo et al., 1996; Souid et al., 2003). This analytical tool assesses bioenergetics in cells undergoing apoptosis (e.g., the mitochondrial cell death pathway), in cells exposed to toxins (e.g., loss of viability) and in cells with a genetically altered energy metabolism (e.g., mitochondrial disorders) (Tacka et al., 2004a-b; Tao et al., 2007; Tao et al., 2008a). This method is applicable to suspended (e.g., Jurkat and HL-60 cells) and adherent (TU183 human oral cancer cells) cells and to fresh tissues from humans (e.g., lymphocytes, spermatozoa and tumors) and animals (e.g., liver, spleen, heart, pancreas and kidney) (Badawy et al., 2009a-b; Whyte et al., 2010; Al Shamsi et al., 2010; Al-Salam et al., 2011; Al Samri et al., 2011). The analyzer allows investigating anticancer compounds (single agents or combinations) for dosing, order of administration and exposure (Jones et al., 2009; Tao et al., 2008b; Souid et al., 2006; Goodisman et al., 2006; Tao et al., 2006a-b; Tack et al. 2004b). It can also be used to monitor reactions consuming or producing O_2 (Tao et al., 2008b; Tao et al., 2009).

2. Relevant biological processes

The term "*cellular bioenergetics*" describes the biochemical processes involved in energy metabolism (energy conversion or transformation), while the term "*cellular respiration*" describes delivery of O_2 to the mitochondria, the breakdown of reduced metabolic fuels with passage of electrons to O_2, and the resulting synthesis of ATP. Impaired respiration thus implies any abnormality involving cellular bioenergetics, including glycolysis. The term "*apoptosis*" describes cellular mechanisms responsible for initiating and executing cell death. The initiation step requires a leakage of cytochrome c from the mitochondrial intermembrane to the cytosol. In the cytosol, cytochrome c binds to the apoptotic protease activating factor-1 (Apaf-1), triggering the caspase cascade (a series of cysteine, aspartate-specific proteases). Caspase activation executes mitochondrial dysfunction (Nicholson et al., 1997). This mitochondrial perturbation involves opening the permeability transition pores (accelerating oxidations in the mitochondrial respiratory chain) and collapsing the

electrochemical potential Δψ (Ricci et al., 2004). Thus, induction of apoptosis is directly linked to mitochondrial dysfunction (Green and Kroemer, 2004).

3. Expressions of dissolved oxygen

Dissolved O_2 is expressed in mm Hg, mL O_2 per L, mg O_2 per L, or μmol per L (μM). For conversion, a partial pressure of O_2 (PO_2) of 1.0 mm Hg = 0.03 mL O_2 per L; 1.0 mL O_2 per L = 1.4276 mg O_2 per L; and 1.0 mg O_2 per L = 1000/32 μM. In *freshwater* at 760 mm Hg and 20°C, dissolved [O_2] is 9.1 mg/L, or 284 μM. Using a Clark electrode, PO_2 of the reaction mixture phosphate-buffer saline (PBS), 10 mM glucose and 0.5% fat-free bovine serum albumin is 170.5 $\pm$ 6.6 mm Hg (n = 4), or 228 $\pm$ 9 μM. The 56 mm Hg difference between [O_2] in freshwater and the reaction solution reflects the effect of salinity on dissolved O_2 (Weiss, 1970).

4. Principles and tools of the oxygen measurement

O_2 concentration is determined from the phosphorescence decay rate ($1/\tau$) of the *palladium (II) complex of meso-tetra-(4-sulfonatophenyl)-tetrabenzoporphyrin* (Pd phosphor). This measurement is based on quenching the phosphorescence of Pd phosphor by O_2 (Lo et al., 1996). The probe has an absorption maximum at 625 nm and an emission maximum at 800 nm. Samples are exposed to light flashes (10 per sec) from a pulsed light-emitting diode array with peak output at 625 nm (OTL630A-5-10-66-E, Opto Technology, Inc), Wheeling, IL. Emitted phosphorescent light is detected by a Hamamatsu photomultiplier tube (PMT #928) after first passing it through a wide-band interference filter centered at 800 nm. Amplified phosphorescence is digitized at 1-2 MHz using an analog/digital converter (PCI-DAS 4020/12 I/O Board) with 1 to 20 MHz outputs (Computer Boards, Inc.). Pulses are captured using a developed software program at 0.1 to 4.0 MHz, depending on speed of the computer (Souid, 2003).

The values of $1/\tau$ are linear with dissolved O_2 concentration: $1/\tau = 1/\tau_o + k_q[O_2]$, where $1/\tau$ = the phosphorescence decay rate in the presence of O_2, $1/\tau_o$ = the phosphorescence decay rate in the absence of O_2, and k_q = the second-order O_2 quenching rate constant in sec^{-1} μM^{-1} (Lo et al., 1996).

Cellular respiration is measured at 37°C in 1-mL sealed vials. Mixing is carried out with the aid of parylene-coated stirring bars. The respiratory substrates are the endogenous metabolic fuels supplemented with glucose. In cell suspensions sealed from air, [O_2] decreased linearly with time, indicating the kinetics of cellular mitochondrial O_2 consumption is zero-order. The rate of respiration (k, in μM O_2 min^{-1}) is thus the negative of the slope d [O_2]/dt. Cyanide markedly inhibited respiration, confirming O_2 is consumed mainly by the mitochondrial respiratory chain.

5. Developed software program and instrument description

The software program was developed using Microsoft Visual Basic 6 (VB6) programming language, Microsoft Access Database 2007 (Access) database management system, and Universal Library components developed by the electronic board company, Measurement Computing, for use with Microsoft Visual Basic 6 programming language

(http://www.mccdaq.com/daq-software/universal-library.aspx). It allows direct reading from the PCI-DAS 4020/12 I/O Board (http://www.mccdaq.com/pci-data-acquisition/PCI-DAS4020-12.aspx). The software utilizes a relational database that stores experiments, pulses and pulse metadata, including slopes. Pulse identification is performed by detecting 10 phosphorescence intensities above 1.0 volt (by default). Peak identification is performed by the program which detects the highest 10% data points of a pulse and chooses the point in the group that is closest to the pulse's decay curve. Depending on the sample rate, a minimum number of data points per pulse is set and used as a cutoff to remove invalid pulses with too few data points (Shaban, 2010).

Main advantages of the developed program over commercially available packages (e.g., DASYLab™ or TracerDAQ™) are provision of full control and customization of the data acquisition, storage and analysis. The choices of VB6 and Access as programming and storage environments are due to their availability, simplicity, widespread use and VB6 components that read directly from the PCI card made available by Measurement Computing. Table 1 displays identified tasks of the program. Fig. 1 shows a picture of the data acquisition system and the developed software program. Fig. 2 shows a reaction vial.

Experiment identification (title, date, time and sample rate)
Reading directly from the PCI card at the fastest possible rate
Distinguishing pulse data from non-pulse data
Allowing a fuzzy detection of the pulse peak
Calculating the exponential decay rate ($1/\tau$) and lifetime (τ) of each pulse
Storing each pulse data points, along with the peak, decay and lifetime values
Viewing a representative pulse every 10 sec
Viewing decay rates ($1/\tau$) in a second graph
Ability to pause and place a marker with a note
Ability to remove erroneous (incomplete) pulses and adjust peak values if necessary
Ability to copy pulse or slope data to clipboard for further analysis
Ability to access a previous experiment, review a pulse with its metadata, markers and associated notes

Table 1. Identified tasks of the customized software program for data acquisition, storage and analysis

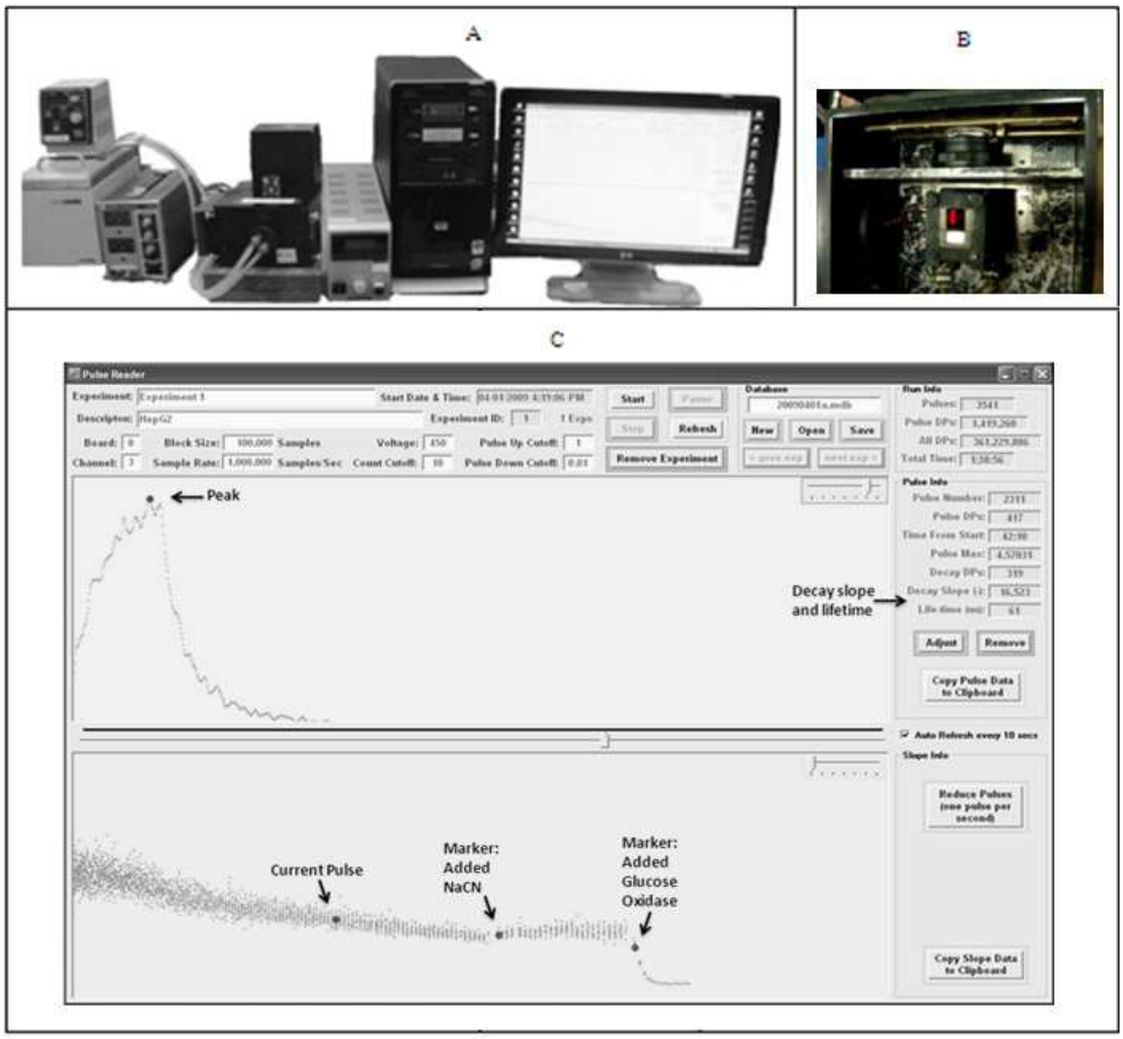

The components (panel A, left to right) are circulating water bath, power supply for the mixer, sample chamber (panel B) attached to PMT, high voltage power supply for PMT, computer with PCI-DAS board, and monitor with developed software running. The PMT is connected to PCI-DAS board on the back of the computer. The developed software program interface is shown in panel C.

Fig. 1. The data acquisition system and developed software program.

Fig. 2. A sealed reaction vial containing Pd phosphor solution, stirring bar and a mouse liver specimen.

6. Instrument calibration

The instrument was calibrated with β-glucose and glucose oxidase system.

$$\beta\text{-glucose} + O_2 \longrightarrow \text{glucono-}\delta\text{-lactone} + H_2O_2$$

The reaction contained PBS, 3 μM Pd phosphor, 0.5% fat-free albumin, 50 μg/mL glucose oxidase and various concentrations of β-glucose. To achieve a high signal-to-nose ratio throughout the entire range of [O_2], the photomultiplier tube was operated at 450 volts. Representative pulses (with exponential fits) for reactions containing PBS with 0, 125 or 500 μM β-glucose, 50 μg/mL glucose oxidase, 3 μM Pd phosphor and 0.5% fat-free bovine serum albumin are shown in Fig. 3.

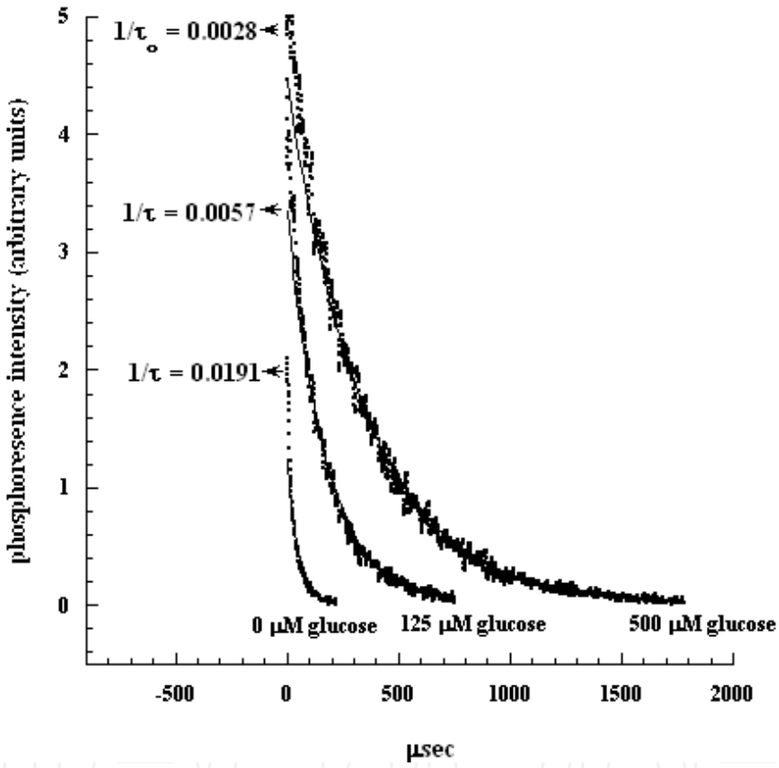

Fig. 3. Representative phosphorescence pulses for reaction mixtures containing 0, 125 or 500 μM glucose. The lines are exponential fits (R^2 >0.924, >0.985 and >0.992, respectively).

The values of $1/\tau$ (mean + SD, n = 1200 over 2 min) as function of [β-glucose] are shown in Fig. 4. The line is linear fit and the value of k_q (101.1 sec^{-1} μM^{-1}) is the negatives of the slope. The value of $1/\tau$ for air-saturated solution (without glucose) was 28,330 sec^{-1} (coefficient of variation, C_v = 12%), for [β-glucose] = 125 μM 5,650 sec^{-1}, and for O_2-depleted solution (with 500 μM β–glucose, $1/\tau_o$) 2,875 sec^{-1} (C_v = 1%). The high values of C_v for the air-saturated solutions were due to the lower phosphorescence intensities with high [O_2] (little light reaching the photomultiplier tube). The corresponding lifetimes (τ) were 52 μsec, 177 μsec and 352 μsec, respectively. Oxygen concentration was calculated using, $1/\tau = 1/\tau_o + k_q[O_2]$.

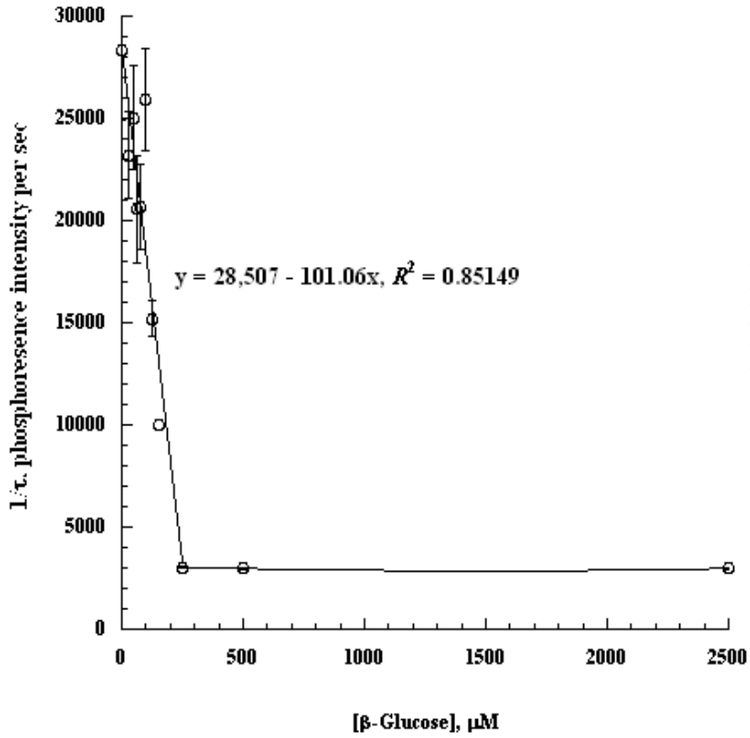

The reaction mixtures contained PBS, 3 μM Pd phosphor, 0.5% fat-free bovine serum albumin, 50 μg/mL glucose oxidase and shown concentrations of β-glucose. The values of $1/\tau$ (mean ± SD, n = 1200 flashes over 2 min) as a function of [β-glucose] are shown. The lines are linear fits.

Fig. 4. Calibration with β-glucose plus glucose oxidase

7. Aflatoxin B1 impairs human lymphocyte respiration

Aflatoxins (most notably, aflatoxin B1) are highly carcinogenic compounds, commonly found in food contaminated by aspergillus flavus, parasiticus and penicillium species (Williams, et al., 2004; Eaton & Gallagher, 1994). These potent mycotoxins create major health problems, especially where food storage is subjected to heat and humidity. A high rate of dietary exposure is reported in Sahara Africa, China and Taiwan. For example, in eastern China (where liver cancer exceeds 1 per 10,000 population per year), an average human exposure to aflatoxins is estimated to be 2.2 μg/kg/day. For comparison, the exposure in the United States is about 3 orders of magnitude less (Wang et al., 1996).

Biotransformation of aflatoxin B1 is critical for its activation. The parent compound undergoes oxidation by monooxygenases, especially the hepatic cytochrome P450 3A4. The active metabolite, AFB exo-8,9-epoxide, undergoes base-catalyzed rearrangement to a dialdehyde, which rapidly reacts with guanyl N7 in DNA and lysine in proteins (Johnson et al., 1996).

Exposure to aflatoxin B1 has been associated with hepatocellular carcinoma (Montesano et al., 1997), mutagenesis (e.g., in the tumor suppressor gene p53) and immune suppression (Corrier, 1991). Most of the information on immunotoxicity of aflatoxin B1 is derived from animal studies (Stec et al., 2009; Reddy et al., 1987; Reddy et al., 1989; Jiang et al., 2008; reviewed in Williams, et al., 2004]. In healthy humans, exposure to aflatoxin B1 is associated

with lower perforin (a cytolytic protein produced by natural killer lymphocytes) expression on CD8+ T-lymphocytes (Jiang et al., 2008). A dose-related decrease in DNA synthesis in lymphocyte cultures (with and without mitogens) is found in mice exposed *in vivo* to aflatoxin B1 (Reddy et al., 1987). A decrease in DNA synthesis is also observed in normal splenic mouse lymphocytes cultured *in vitro* with >10 μM aflatoxin B1; a decrease in RNA synthesis is observed at dosing >25 μM and a decrease in protein synthesis at dosing >100 μM (Reddy et al., 1989).

The phosphorescence oxygen analyzer is used to monitor the effects of aflatoxin B1 on human lymphocyte mitochondrial oxygen consumption. These experiments investigate whether aflatoxin B1 impairs respiration of the lymphoid tissue, an organ that is typically targeted by this potent mycotoxin. Aflatoxin B1 (1.0 mg = 3.2 micromol) was freshly dissolved in 1.0 mL dry methanol and immediately added to cell suspensions with vigorous mixing. Alternatively, aflatoxin B1 powder was directly added to the cell suspension with vigorous mixing. The concentrations were determined by the absorbance at 350 nm (10 μL aflatoxin B1 stock solution or cell-free supernatant in 1.0 mL dry methanol), using an extinction coefficient of 21,500 M^{-1} cm^{-1} (Nesheim et al., 1999); the aflatoxin B1 excitation wavelength is 366 nm and the emission wavelength 455 nm. The reactions were carried out in glass vials and protected from light.

PBMC (0.6 x 10^7 cells/mL) were suspended in 6.0 mL PBS, 10 mM glucose, 3 μM Pd phosphor and 0.5% fat-free bovine serum albumin. The mixture was divided into 2 equal aliquots. Methanol (25 μL per mL, Fig. 5, left panel) or aflatoxin B1 (25 μM, Fig. 5, right panel) was then added and the incubation continued at 37°C (open to air with gentle stirring). At t = 10 and 110 min, 1.0 mL of each mixture was simultaneously placed in the instruments for O_2 measurement. The rate of respiration (k, in μM O_2 min^{-1}) for t = 10 to 78 min for the methanol-treated cells was 2.0 and for the aflatoxin B1-treated cells 2.1. The values of k for t = 110 to 174 were 2.2 and 1.2, respectively (corresponding to 45% inhibition of lymphocyte respiration).

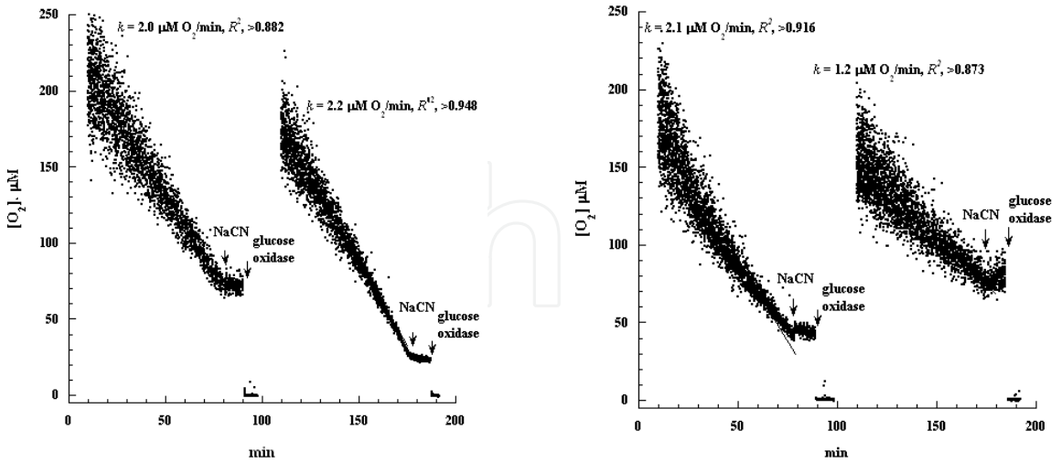

PBMC were incubated at 37°C with 25 μL per mL methanol (left panel) or 25 μM aflatoxin B1 (right panel). Minute zero corresponds to the addition of aflatoxin B1. At t = 10 and t = 110 min, 1.0 mL of each mixture was simultaneously placed in the instruments for O_2 measurement. Rates of respiration (k) were calculated from the best-fit linear curves. Additions of 5.0 mM NaCN and 50 μg/mL glucose oxidase are shown.

Fig. 5. Effect of aflatoxin B1 on human PBMC respiration.

The time-course for aflatoxin B1-induced inhibition of lymphocyte respiration was investigated (Fig. 6). PBMC (1.3 x 10^7 cells/mL) were suspended in 3.0 mL PBS, 10 mM glucose and divided into 2 equal aliquots. Aflatoxin B1 powder was directly added to one aliquot with vigorous mixing (final concentration, ~75 μM). The 2 aliquots were then incubated at 37°C for 60 min (open to air with continuous stirring). At t = 60 min, 5 mg albumin and 2.0 μM Pd phosphor were added to each suspension. The samples were then simultaneously placed in the chambers for O_2 measurement. For the untreated cells, O_2 consumption was linear with time (k = 2.4 μM O_2/min, $R^2 > 0.916$). For the treated cells, O_2 consumption was exponential with time, $R^2 > 0.934$. Changes at 5-min intervals for the treated cells showed a sharp decline in the values of k for t = 60 to 90 min, followed by a steady low rate for t = 95 to 175 min. In contrast, the values of k remained relatively stable for t = 60 to 140 min. The mean ± SD (coefficient of variation) for the values of k for the untreated cells was 2.43 ± 0.55 (C_v = 23%) and for the treated cells 1.56 ± 1.80 (C_v = 87%); p-value < 0.02 (Fig. 6, insert).

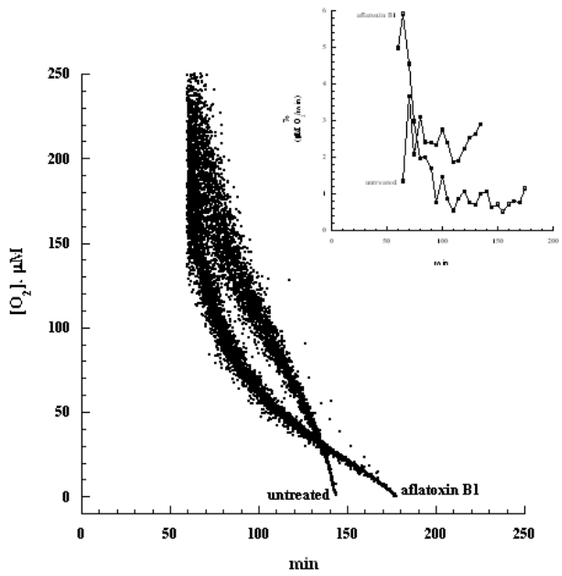

The lines are linear fit for the untreated cells ($R^2 > 0.916$) and exponential fit for the treated cells ($R^2 > 0.936$). Insert, changes in the values of k at 5-min intervals.

Fig. 6. Time-course of the effect of aflatoxin B1 on human lymphocyte respiration.

The exponential profile of O_2 consumption in the presence of aflatoxin B1 is similar to dactinomycin (Tao et al., 2006b; Tao et al., 2008a). This pattern of bioenergetic derangements could stem from progressive mitochondrial and metabolic disturbances, ranging from uncoupling oxidative phosphorylation (which accelerates O_2 consumption and rapidly depletes the metabolic fuels) to mitochondrial respiratory chain function collapse. Experimentally, these two phases are clearly distinguishable in our system (Fig. 6, insert).

Caspase activation in lymphocytes treated with aflatoxin B1 was then examined. Many of the caspases (e.g., caspase-3, -2 and -7) target the asp-glu-Val-asp (DEVD) motif and cleave at sites next to the last aspartate residue (Nicholson et al., 1997). Synthetic cell-permeable substrates, such as N-acetyl-DEVD-7-amino-4-trifluoromethyl coumarin (Ac-DEVD-AFC) and N-acetyl-DEVD-7-amino-4-methyl coumarin (Ac-DEVD-AMC) have been used to investigate caspase activities. For example, cleavage of Ac-DEVD-AFC by specific caspases

releases the fluorogenic AFC; the latter can be separated on HPLC and detected by fluorescence with a great sensitivity (Tao et al., 2007).

Caspase-3 activity in lymphocytes exposed to aflatoxin B1 is shown in Fig. 7. The purpose of these experiments is to confirm caspases are activated within the time period required for inhibition of respiration. The mixtures (final volume, 0.5 mL) contained 1.5 x 10^6 cells in PBS, 10 mM glucose and 68 μM Ac-DEVD-AMC (N-acetyl-asp-glu-val-asp-7-amino-4-methyl coumarin, a caspase-3 substrate) with and without 20 μM zVAD-fmk (benzyloxycarbonyl-val-ala-DL-asp-fluoromethylketone, a pan-caspase inhibitor) (Slee et al., 1996). The suspensions were incubated at 37°C for 2 hr without other additions (Fig. 7, left panel) or with the addition of ~100 μM aflatoxin B1 (Fig. 7, right panel). At the end of the incubation period, the cells were disrupted and their supernatants were separated on HPLC and monitored by fluorescence. The results show AMC moieties (the cleavage product of Ac-DEVD-AMC) appear in the cells about 2 hr after the addition of aflatoxin B1. This 2-hr period is the same as that observed for aflatoxin B1-induced inhibition of respiration (see Fig. 5). Thus, the results suggest aflatoxin B1 impairs human lymphocyte mitochondrial function by activating caspases.

The above findings also demonstrate the lymphocyte preparation contain monooxygenases that activate aflatoxin B1. These results are consistent with previous reports (Stec et al., 2009; Rossano et al., 1999; Savel et al., 1970; Wang et al., 1999). In one study, the addition of aflatoxins B1 at concentrations up to 32 μM had a minimum effect on phytohemagglutinin-p-stimulated human lymphocyte proliferation (Meky et al., 2001). However, an earlier study on human lymphocytes by Savel et al. (1970) showed a reduced phytohemagglutinin-p-stimulated lymphocyte proliferation with 16 μM aflatoxin B1. More recently, aflatoxin B1 was shown to inhibit *in vitro* concanavalin A-induced proliferation of pig blood lymphocytes; in 72-hr cultures, the concentration of aflatoxin B1 producing 50% inhibition (IC_{50}) was 60 nM (Stec et al., 2009). In other studies, aflatoxin G1 induced *in vitro* apoptosis in human lymphocytes (Wang et al., 1999; Sun et al., 2002). In summary, the data presented show human lymphocytes exposed *in vitro* to aflatoxin B1 exhibit impairments of cellular respiration, which could result from caspase activation. The results substantiate the potent immunosuppressive activity of aflatoxins in human.

8. Measurement of O_2 consumption in murine tissues

A novel *in vitro* system is developed to measure O_2 consumption by various murine tissues over several hours (Al-Salam et al., 2011; Al Samri et al., 2011; Al Shamsi et al., 2010). Small tissue specimens excised from male Balb/c mice were immediately immersed in ice-cold Krebs-Henseleit buffer (115 mM NaCL, 25 mM $NaHCO_3$, 1.23 mM NaH_2PO_4, 1.2 mM Na_2SO_4, 5.9 mM KCL, 1.25 mM $CaCl_2$, 1.18 mM $MgCl_2$ and 6 mM glucose, pH ~7.4), saturated with 95% O_2:5% CO_2. The samples were incubated at 37°C in the same buffer and continuously gassed with O_2:CO_2 (95:5). Normal tissue histology at hr 5 was confirmed by light and electron microscopy. NaCN inhibited O_2 consumption, confirming the oxidation occurred in the mitochondrial respiratory chain. A representative experiment of pneumatocyte respiration is shown in Fig. 8. The rate of lung tissue respiration incubated *in vitro* for 3.9 < t <12.4 hr was 0.24 ± 0.03 μM O_2 min^{-1} mg^{-1} (mean ± SD, n = 28). The corresponding rate for the liver was 0.27 ± 0.13 (n = 11, t <4.7 hr), spleen 0.28 ± 0.07 (t <5 hr, n = 10), kidney 0.34 ± 0.12 (t <5 hr, n = 7) and pancreas 0.35 ± 0.09 (t <4 hr, n = 10), Table 2. This approach provided accurate assessment of tissue bioenergetics *in vitro* over several hours.

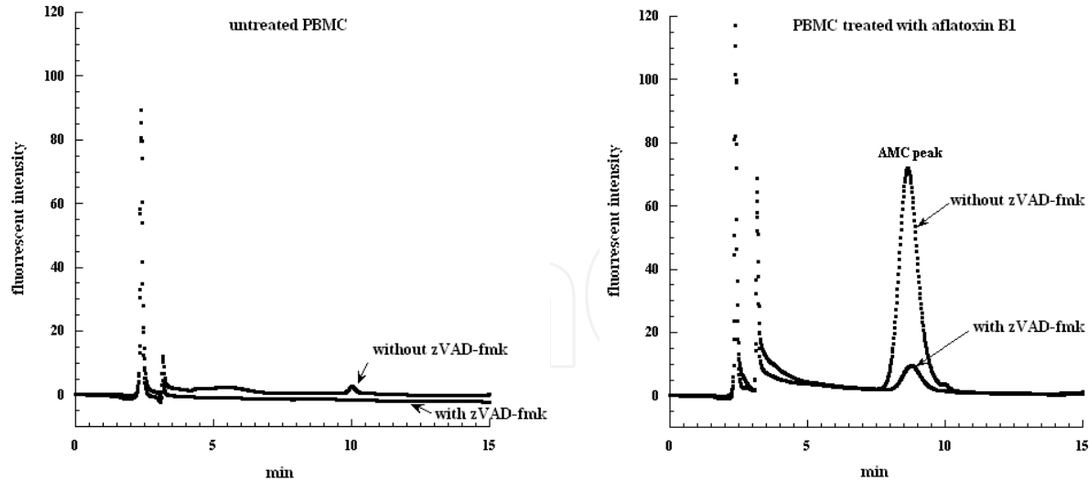

The reactions contained 1.5 x 10^6 cells in PBS plus 10 mM glucose and 68 μM Ac-DEVD-AMC with and without 20 μM zVAD-fmk. The suspensions were incubated at 37°C for 2 hr without other additions (left panel) or with the addition of ~100 μM aflatoxin (right panel). At the end of the incubation period, the cells were disrupted and their supernatants were separated on HPLC and monitored by fluorescence. The retention time for Ac-DEVD-AMC was ~2.4 min and for the released AMC ~8.7 min.

Fig. 7. Caspase activation by aflatoxin B1 in human peripheral blood mononuclear cells parenthesis for PBMC:PBMC

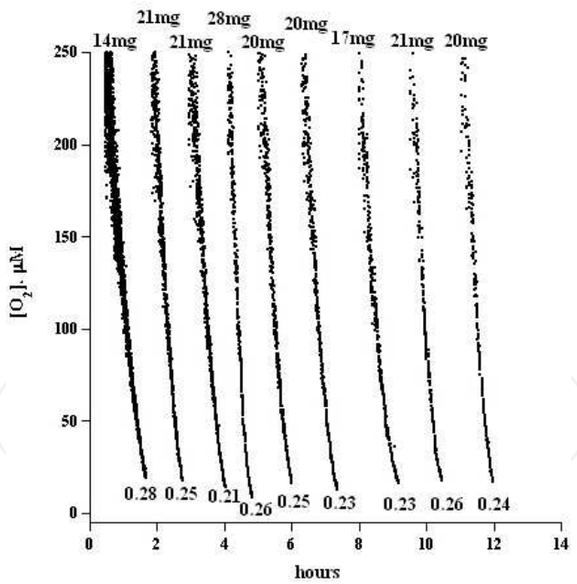

Specimens were excised from the lung of an anesthetized mouse and immediately immersed in ice-cold Krebs-Henseleit buffer saturated with 95% O_2:5% CO_2. The samples were incubated at 37°C in the same buffer with continuous gassing with O_2:5%CO_2. At indicated time periods, specimens were removed from the incubation mixture, weighed and placed in Krebs-Henseleit buffer containing 0.5% albumin and 3 μM Pd phosphor for O_2 measurement. The rate of respiration was set as the negative of the slope of [O_2] vs. time. The weight is shown at the top and the respiration rate (in μM O_2 min^{-1} mg^{-1}) at the bottom of each run (Al Samri et al., 2011).

Fig. 8. Representative experiment of O_2 consumption by lung tissue.

Tissues	Respiration ($\mu M\ O_2\ min^{-1}\ mg^{-1}$)
Lung	0.24 ± 0.03
Liver	0.27 ± 0.13
Spleen	0.28 ± 0.07
Kidney	0.34 ± 0.12
Pancreas	0.35 ± 0.09

Values are mean ± SD. For unit conversion, 1.0 mL O_2 = 1.4276 mg or 0.0446125 mmol.

Table 2. O_2 consumption by murine tissues.

9. Biocompatibility of calcined mesoporous silica particles with murine tissue bioenergetics

The *in vitro* system discussed in Section 8 is used to investigate the effects of two forms of calcined mesoporous silica particles (MCM41-cal and SBA15-cal) on cellular respiration of mouse tissues (Al Shamsi et al., 2010; Al-Salam et al., 2011; Tao et al., 2008c). O_2 consumption by lung, liver, kidney, spleen and pancreatic tissues was unaffected by exposure to 200 μg/mL MCM41-cal or SBA15-cal for several hours. A representative experiment of pneumatocyte respiration is shown in Fig. 9.

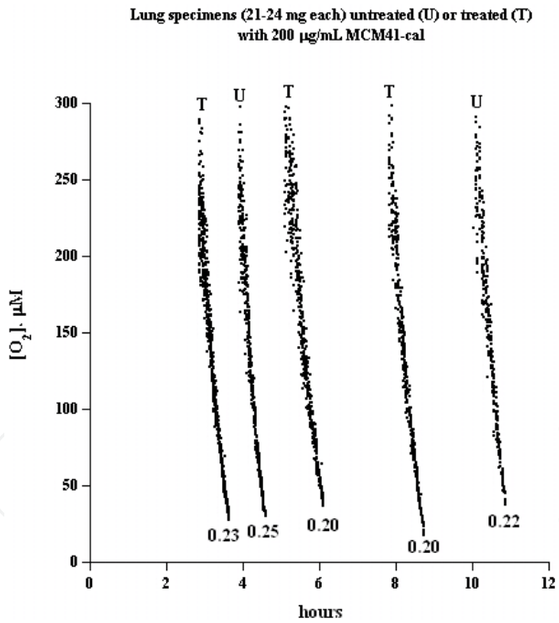

The rate of respiration (k) was set as negative of the slope of [O_2] vs. time; the values of k (in $\mu M\ O_2\ min^{-1}\ mg^{-1}$) are shown at the bottom of the runs. Zero minute corresponds to the addition of the particles. U, untreated; and T, treated.

Fig. 9. Pneumatocyte respiration with and without 200 μg/mL MCM41-cal.

Normal tissue architecture and histology were confirmed by light microscopy. Intracellular accumulation of the particles in the studied tissues was evident by electron microscopy. The results show reasonable *in vitro* biocompatibility of the mesoporous silicas with murine

tissue bioenergetics. Therefore, the measurements of respiration can be used to explore biocompatibility and viability of tissues and cells as a result of various treatments.

10. Liver tissue bioenergetics in concanavalin A hepatitis in mice

Concanavalin A (Con A) is a plant lectin from the seeds of Canavalia ensiformis (jack bean). This toxin serves as a polyclonal T-cell mitogen. It produces fulminant hepatitis in mice, a disease that mimics human infection with hepatitis B virus (Tiegs et al., 1992 & 1997). The hepatic injury is typically noted within 3 hr of intravenous injection of > 1.5 mg/kg of Con A and progresses with time (Tiegs et al., 1992). Activation and recruitment of Natural Killer (NK) T-cells and other cells of the innate immune system are early events, which lead to increased secretion of various inflammatory cytokines (e.g., TNF-α, IL-2, IL-10, IL-12 and IFN-γ) (Takeda et al., 2000; Margalit et al., 2005; Chen et al., 2010; Sass et al., 2002). This immune response targets multiple organs including the liver. Its outcome is irreversible hepatotoxicity, which includes inflammatory infiltrates and necrosis (Leist et al., 1996).

The above described *in vitro* system is employed to assess liver tissue respiration in Con A treated C57BL/6 mice. The purpose of the work was to estimate hepatocyte bioenergetics in this well-studied hepatitis model. The mice were injected intravenously with 12 mg/kg Con A or PBS. Specimens (20 to 30 mg each) were cut from the liver of anesthetized (urethane, 100 μL per 10 g body weight, using 25% solution, w/v, in 0.9% NaCl) mice using a sharp scissor (Moria Vannas Wolg Spring, cat. # ST15024-10) (Al Samri et al., 2011). The specimens were immediately immersed in ice-cold Krebs-Henseleit buffer (115 mM NaCl, 25 mM $NaHCO_3$, 1.23 mM NaH_2PO_4, 1.2 mM Na_2SO_4, 5.9 mM KCl, 1.25 mM $CaCl_2$, 1.18 mM $MgCl_2$ and 6 mM glucose, pH ~7.2), gassed with 95% O_2:5% CO_2. Pieces were then weighed and placed in 1-ml Pd phosphor solution (Krebes-Henseleit buffer containing 0.5% albumin and 3 μM Pd phosphor) for O_2 measurement. The results are summarized in Table 3.

Strain	Treatment	k_c (μM O_2 min^{-1} mg^{-1})	
		mean ± SD (n)	range
C57Bl/6	PBS	0.26 + 0.04 (5)	0.22 – 0.32
	12 mg/kg Con A	0.18 + 0.03 (5)*	0.13 – 0.20

* *P*-value = 0.005

Table 3. Liver tissue respiration in Con A treated C57BL/6 mice. Mice were injected with Con A or PBS. Liver specimens were collected 12 hr post injection.

A representative experiment following 3-hr treatment is shown in Fig. 10. Liver tissue respiration was measured 3 hr post injection of PBS (Fig. 10, left panel) or 12 mg/kg Con A (Fig. 10, right panel). In untreated mouse, the rates of respiration at t = 0 min and t = 80 min (post tissue collection) were similar. In Con A-treated mouse, the rate of respiration at t = 0 min was high and at t = 40 min it was low. Thus, at 3-hr, Con A treatment doubled the rate of liver tissue O_2 consumption. However, respiration deteriorated *in vitro* in 40 min.

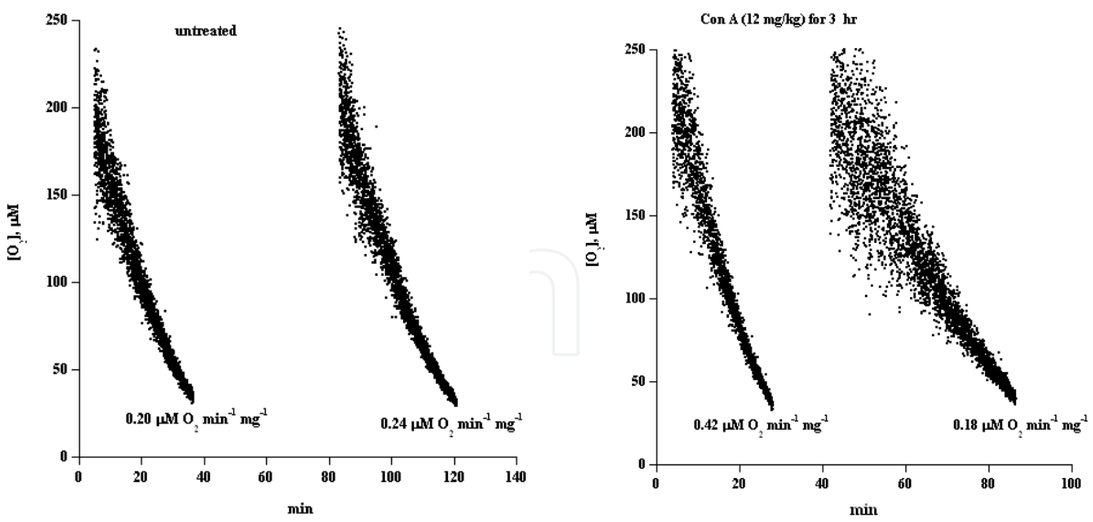

Minutes zero correspond to collecting the liver tissue specimens at 3 hr post injections. Two runs were done for each condition. Rates of respiration (k_c, in µM O_2 min^{-1} mg^{-1}) are shown at the bottom of the runs.

Fig. 10. Representative experiment for liver tissue respiration in C57BL/6 mice 3 hr post injection of PBS (left panel) or 12 mg/kg Con A (right panel)

Thus, Con A treatment produced a concurrent impairment of hepatocyte respiration. The lower rate of respiration at 12 hr post treatment (Table 3) concurred with large areas of necrosis and the enhanced rate of respiration at ~3 hr post treatment (Fig. 10) concurred with inflammatory infiltrates limited to the perivascular space without any notable necrosis. The latter finding suggests a role for inflammatory mediators, such as TNF-α and IL-2 (both known to peak 3 hr post Con A treatment) in modulating hepatocyte energy metabolism (Louis et al., 1997; Gottlieb et al., 2000). The mechanism for the presumed inflammation-induced increase in hepatocyte oxygen consumption could be uncoupling oxidative phosphorylation *vs.* up-regulating the energy metabolism. Nevertheless, for both assumptions, there is a large demand for energy supply to prevent fulminant liver necrosis.
In an *in vitro* experiment, liver tissue respiration was measured with and without IL-2 (added directly to the O_2 measuring vial). The rate of respiration without IL-2 was 0.21 µM O_2 min^{-1} mg^{-1} and with IL-2 0.087 µM O_2 min^{-1} mg^{-1} (~60% inhibition). Thus, similar to TNF-α, IL-2 also inhibits cellular respiration *in vitro* (Gottlieb et al., 2000).

11. Spermatozoa respiration

The above *in vitro* system was also used to measure human spermatozoa respiration. O_2 concentrations in solutions containing glucose and human spermatozoa declined linearly with time. Sodium cyanide also inhibited sperm oxygen consumption, confirming the oxidations occurred in the respiratory chain. The rate of respiration (mean $\pm$ SD, n = 10) was 1.0 $\pm$ 0.3 µM O_2 min^{-1} per 10^8 sperm. Immediate decline in the rate of sperm respiration was noted when toxic agents [e.g., 4-hydroperoxycyclophosphamide (4OOH-CP), Δ^9-tetrahydrocannabinol (Δ^9-THC) or Δ^8-tetrahydrocannabinol (Δ^8-THC)] were added to washed sperm or neat semen. The inhibition was concentration-dependent and irreversible (Badawy et al., 2009a-b).

The toxic effect of the cannabinoids was confirmed on isolated mitochondria from beef heart. The effect of Δ^8-THC on respiration of beef heart mitochondria is shown in Fig. 11. The value of k (in μM O_2 min^{-1}) decreased by 64% in the presence of 240 μM Δ^8-THC.

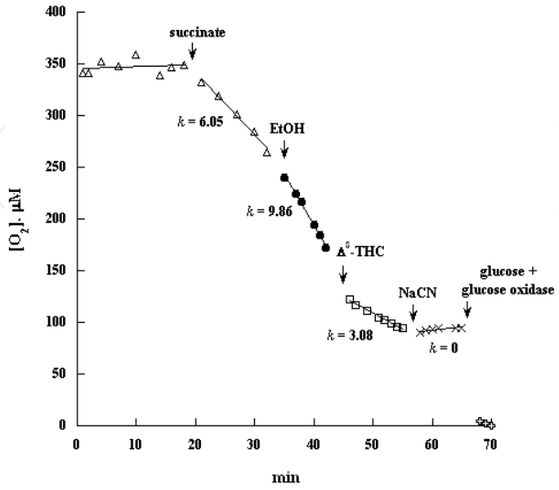

Fig. 11. Δ^8-THC added to isolated mitochondria from beef heart.

12. Phosphorescence O_2 analyzer as a screening tool for disorders of impaired cellular bioenergetics

Disorders of cellular bioenergetics are challenging clinically and biochemically (Chretien and Rustin, 2003; Chretien et al., 1994; Rotig et al., 1990; Rustin et al., 1994). Their manifestations frequently overlap with numerous clinical entities. Furthermore, mutations that limit these processes in humans are incompletely identified (http://www.gen.emory.edu/mitomap.html) (Kogelnik et al., 1997). Therefore, clinicians usually rely on a laborious analysis of skin and muscle biopsies for diagnosis (Chretien and Rustin, 2003; Chretien et al., 1994; Rustin et al., 1994). As suggested by Rustin et al., laboratory evaluation of mitochondrial disorders require testing samples from multiple tissues. The authors also recommended the use of circulating lymphocytes in the initial screening (Rustin et al., 1994). These interrelations justify developing non-invasive simple screening methods that are applicable to various types of samples. Recently, Marriage et al. showed ATP synthesis in permeabilized lymphocytes is an effective screening tool for impaired oxidative phosphorylation (Marriage et al., 2003; Marriage et al., 2004). Decreased ATP synthesis in the lymphocytes was present in the 5 studied mitochondrial disorders (Marriage et al., 2003).

Described herein is the use of the phosphorescence O_2 analyzer to measure lymphocyte respiration in volunteers and a patient. The measurement primarily aimed to show feasibility of using the phosphorescence O_2 analyzer to screen for clinical disorders with impaired cellular bioenergetics. Peripheral blood mononuclear cells (PBMC) were collected from healthy volunteers and patient. The rate of respiration (mean ± SD, in μM O_2 per min per 10^7 cells) for adult volunteers is 2.1 ± 0.8 (n = 18), for children 2.0 ± 0.9 (n = 20), and for newborns (umbilical cord samples) 0.8 ± 0.4 (n = 18, p <0.0001). Representative experiments of the volunteers are shown in Fig. 12.

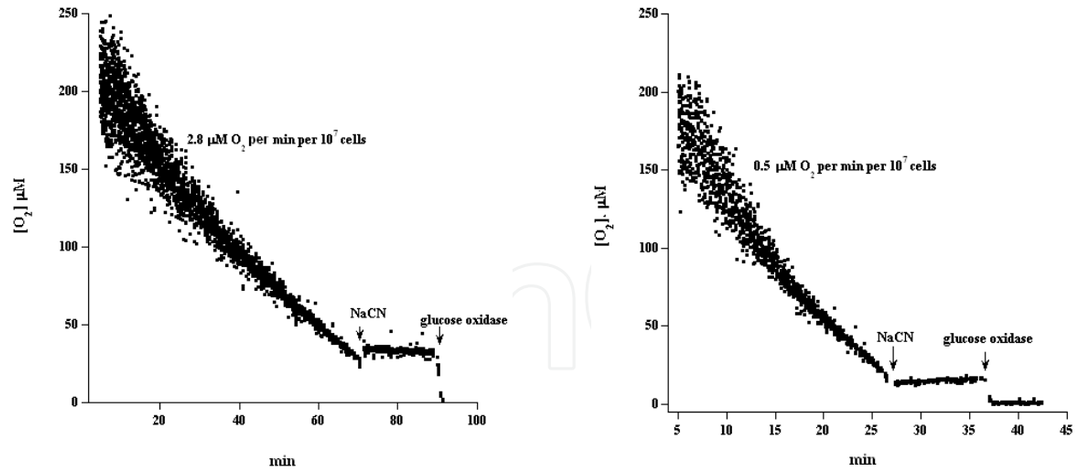

Fig. 12. Left panel: Lymphocytes (1.0 x 10^7 cells/mL) were collected from a 9-year-old girl; the rate of respiration was 2.8 μM O_2 per min per 10^7 cells (R^2 >0.942). Right panel: Lymphocytes (15 x 10^7 cells/mL) were collected from umbilical cord; the rate of respiration was 8.0 μM O_2 per min (R^2 >0.934), or 0.5 μM O_2 per min per 10^7 cells. The additions of 5.0 mM NaCN and 50 μg/mL glucose oxidase are shown.

For an 8-year-old patient with reduced muscle NADH dehydrogenase and pyruvate dehydrogenase activities, the rate was 0.7 ± 0.2 (n = 3) μM O_2 per min per 10^7 cells.

As previously noted in muscle specimens, the rate of lymphocyte mitochondrial oxygen consumption is very similar in adults and children (p =0.801) (Chretien et al., 1994). However, cord blood cells have lower rates of respiration (p <0.001). This finding could be attributed to the high number of nucleated red blood cells in the umbilical cord blood.

Fresh lymphocytes were previously used as a source of tissue for measuring respiratory chain enzymes by polarography (Clark-type O_2 electrode) and spectroscopy (Chretien and Rustin, 2003; Chretien et al., 1994; Rustin et al., 1994). Rotig et al. reported a rate (mean + SD, n=15) of 3.5 $\pm$ 0.5 nmol O_2 per min per 10^7 cells (Rotig et al., 1990). Hedeskov and Esmann reported a rate of 2.0 $\pm$ 0.07 nmol O_2 per min per 10^7 for cell concentrations >4 x 10^7 per mL and higher rates for less concentrated cells (Hedeskov and Esmann, 1966). Pachman reported rate of 1.0 $\pm$ 0.2 nmol O_2 per min per 10^7 equine lymphocytes (Pachman, 1967).

Clinical presentations of entities with impaired cellular bioenergetics vary markedly. Their manifestations may include progressive neuromuscular defects (e.g., psychomotor retardation and hypotonia), heart muscle involvement and encephalopathy. One typical example is Leigh syndrome, which results from an isolated mitochondrial complex I deficiency (Benit et al., 2004). This clinical heterogeneity stems from various mechanisms, including tissue-specific of nuclear-encoded isoforms of the respiratory chain and existence of normal and mutated mtDNA in the same organ (mtDNA heteroplasmy) (Rustin et al., 1994). Therefore, as suggested by Rustin et al., the biochemical analysis should not be limited to skeletal muscle and skin tissues (Rustin et al., 1994). In one study, 42 patients with respiratory chain defects were investigated. The results showed that 50% of the patients had deficiencies in skeletal muscles and lymphocytes, 45% in skeletal muscles only, and 5% in lymphocytes only (Chretien et al., 1994). Patients with Pearson's syndrome on the other hand consistently express defects in the lymphocyte (Rotig et al., 1990).

13. Conclusions

A novel *in vitro* system that allows monitoring of cellular respiration over several hours is described. The method has numerous biological applications, including studying mitochondrial dysfunction during apoptosis or toxic exposure. It also allows screening for metabolic disorders in patients. The procedure is sensitive and reproducible. It is applicable to cells in suspension, adherent cells and various organs, including the heart muscle, liver, spleen, pancreas and kidney.

14. References

Al-Salam, S.; Balhaj, G.; Al-Hammadi, S.; Sudhadevi, M.; Tariq, S.; Biradar, A.V.; Asefa, T. & Souid, A.-K. (2011). *In vitro* study of calcined mesoporous silica nanoparticles in mouse lung. *Toxicology Sciences*. Vol.122, No.1, (Epub 2011 Apr 5), pp.86-99.

Al Samri, M.T.; Al Shamsi, M.; Al-Salam, S.; Marzouqi, F.; Mansouri, A.; Al-Hammadi, S.; Balhaj, G.; Al Dawaar, S.K.M.; Al Hanjeri, R.S.M.S.; Benedict, S.; Sudhadevi, M.; Conca, W.; Penefsky, H.S. & Souid, A.-K. (2011). Measurement of oxygen consumption by murine tissues *in vitro*. *Journal of Pharmacological and Toxicological Methods*. Vol.63, No.2, (Epub 2010 Oct 27), pp.196-204.

Al Shamsi, M.; Al Samri, M.T.; Al-Salam, S.; Conca, W.; Shaban, S.; Benedict, S.; Tariq, S.; Biradar, A.; Penefsky, H.S.; Asefa, T.; Souid, A.-K. (2010). Biocompatibility of calcined mesoporous silica particles with cellular bioenergetics in murine tissues. *Chemical Research in Toxicology*. Vol.23, No.11, (Epub 2010 Oct 20), pp.1796-1805.

Badawy, Z.S. & Souid, A.-K. (2009a). Inhibition of human sperm respiration by 4-hydroperoxycyclophosphamide and protection by mesna and WR-1065. *Fertility and Sterility*. Vol.91, No.1, (2008 Jan 18), pp.173-178.

Badawy, Z.S.; Chohan, K.R.; Whyte, D.A.; Penefsky, H.S.; Brown, O.M. & Souid, A.-K. (2009b). Cannabinoids inhibit the respiration of human sperm. *Fertility and Sterility*. Vol.91, No.6, (2008 Jun 18), pp.2471-2476.

Benit, P.; Slama, A.; Cartault, F.; Giurgea, I.; Chretien, D.; Lebon, S.; Marsac, C.; Munnich, A.; Rotig, A. & Rustin, P. (2004). Mutant NDUFS3 subunit of mitochondrial complex I causes Leigh syndrome. *Journal Medical Genetics*. Vol.41, No.1, pp.14-17.

Chen, F.; Zhu, H-H.; Zhou, L-F.; Li, J.; Zhao, L-Y.; Wu, S-S.; Wang, J.; Liu, W. & Chen, Z. (2010). Genes related to the very early stage of ConA-induced fulminant hepatitis: a gene-chip-based study in a mouse model. *BMC Genomics*. Vol.11, pp.240-250.

Chretien, D.; Rustin, P.; Bourgeron, T.; Rotig, A.; Saudubrary, J.M. & Munnich, A. (1994). Reference charts for respiratory chain activities in human tissues. *Clin. Chim. Acta*. Vol.228, No.1, pp.53-70.

Chretien, D. & Rustin, P. (2003). Mitochondrial oxidative phosphorylation: pitfalls and tips in measuring and interpreting enzyme activities. *J. Inherit. Metab. Dis*. Vol.26, No.(2-3), pp.189-198.

Corrier, DE. (1991). Mycotoxicosis: mechanisms of immunosuppression. *Vet Immunol Immunopathol*. Vol.30, No.1, pp.73-87.

Eaton, D.L. & Gallagher, E.P. (1994). Mechanisms of aflatoxin carcinogenesis. *Annu. Rev. Pharmacol. Toxicol*. Vol.34, pp.135-172.

Goodisman, J.; Hagrman, D.; Tacka, KA. & Souid, A-K. (2006). Analysis of cytotoxicities of platinum compounds. *Cancer Chemotherapy and Pharmacology*. Vol.57, No.2, (2005 Jul 19). pp.257-267.

Gottlieb, E.; Vander Heiden, MG. & Thompson, CB. (2000). Bcl-xL Prevents the Initial Decrease in Mitochondrial Membrane Potential and Subsequent Reactive Oxygen Species Production during Tumor Necrosis Factor Alpha-Induced Apoptosis. *Molecular and Cellular Biology*. Vol.20, No.15. pp.5680–5689.

Green, D.R. & Kroemer, G. (2004). The pathophysiology of mitochondrial cell death. *Science*. Vol.305, No.5684. pp. 626-629.

Hedeskov, C.J. & Esmann, V. (1966). Respiration and glycolysis of normal human lymphocytes. *Blood*. Vol.28, No.2. pp. 163-174.

Jiang, Y.; Jolly, P.E.; Preko, P.; Wang, J-S.; Ellis, W.O.; Phillips, T.D. & Williams, J.H. (2008). Aflatoxin-related immune dysfunction in health and in human immunodeficiency virus disease. *Clin. Dev. Immunol*. (2008:790309).

Johnson, WW.; Harris, T.M. & Guengerich, FP. (1996) Kinetics and mechanism of hydrolysis of aflatoxin B1 exo-8, 9-Epoxide and rearrangement of the dihydrodiol. J Am Chem Soc. Vol.118, No.35, pp.8213-8220.

Jones, E.; Penefsky, HS. & Souid A-K. (2009). Caffeine impairs HL-60 cellular respiration. *Journal of Medical Sciences*. Vol.2, No.2, pp. 61-72.

Kogelnik, A.M.; Lott, M.T.; Brown, M.D.; Navathe, S.B. & Wallace, D.C. (1997). MITOMAP: an update on the status of the human mitochondrial genome database. *Nucleic Acids Res*. Vol.25, No.1, pp. 196-199.

Leist, M. & Wendel, A. (1996). A novel mechanism of murine hepatocyte death inducible by concanavalin A. *J Hepatol*. Vol.25, No.6, pp.948-959.

Lo L-W, Koch CJ, Wilson DF (1996). Calibration of oxygen-dependent quenching of the phosphorescence of Pd-meso-tetra (4-carboxyphenyl) porphine: A phosphor with general application for measuring oxygen concentration in biological systems. *Analytical Biochemistry*. Vol.236, No.1, pp.153-160.

Louis H, Moine O L, Peny M-O, Quertinmont E, Fokan D, Goldman M & Devie`re J. (1997). Production and role of interleukin-10 in concanavalin A–induced hepatitis in mice. *Hepatology*. Vol.25, No.6, pp.1382-1389.

Margalit, M.; Abu Ghazala, S.; Alper, R.; Elinav, E.; Klein, A.; Doviner, V.; Sherman. Y.; Thalenfeld, B.; Engelhardt, D.; Rabbani, E. & Ilan, Y. (2005). Glucocerbroside treatment ameliorates conA hepatitis by inhibition of NKT lymphocytes. *Am J Physiol Gastrointest Liver Physiol*. Vol.289. No.5, (Epub 2005 Jun 23), pp.G917-25.

Marriage, B.J.; Clandinin, M.T.; MacDonald, IM. & Glerum, D.M. (2003). The use of lymphocytes to screen for oxidative phosphorylation disorders. *Analytical Biochemistry*. Vol.313, No.1, pp.137-144.

Marriage, B.J.; Clandinin, M.T.; MacDonald, I.M. & Glenerum D.M. (2004). Cofactor treatment improves ATP synthetic capacity in patients with oxidative phosphorylation disorders. *Molecular Genetics Metabolism*. Vol..81, No.4, pp.263-272.

Meky, F.A.; Hardie, L.J.; Evans, S.W. & Wild, C.P. (2001). Deoxynivalenol-induced immunomodulation of human lymphocyte proliferation and cytokine production. *Food Chem. Toxicol*. Vol.39, No.8, pp.827-836.

Montesano, R.; Hainaut, P. & Wild, C.P. (1997). Hepatocellular carcinoma: from gene to public health. *J. Natl. Cancer Inst*. Vol..89, No.24, pp.1844-1851.

Nesheim, S.; Trucksess, M.W. & Page, S.W. (1999). Collaborative study, molar absorptivities of aflatoxins B1, B2, G1, and G2 in acetonitrile, methanol and toluene-acetonitrile (9+1) (modification of AOAC official method 971.22). *J. AOAC Int*. Vol.82, No.2, pp.251-258.

Nicholson, D.W. & Thornberry, N.A. (1997). Caspases: killer proteases. *Trends Biochem Sci*. Vol.22, No.8, pp.299-306.

Pachman L.M. (1967). The carbohydrate metabolism and respiration of isolated small lymphocytes. In vitro studies of normal and phytohemagglutinin stimulated cells. *Blood*. Vol.30, No.6, pp.691-706.

Reddy, R.V.; Taylor, M.J. & Sharma, R.P. (1987). Studies of immune function of CD-1 mice exposed to aflatoxin B1. *Toxicology*. Vol.43, No.2, pp.123-132.

Reddy, R.V. & Sharma, R.P. (1989). Effects of aflatoxin B1 on murine lymphocyte functions. *Toxicology*. Vol.54, No.1, pp.31-44.

Ricci, J-E.; Munoz-Pinedo, C.; Fitzgerald, P.; Bailly-Maitre, B.; Perkins, GA.; Yadava, N.; Scheffer, IE.; Ellisman, MH. & Green, DR. (2004). Disruption of mitochondrial function during apoptosis is mediated by caspase cleavage of the p75 subunit of complex I of the electron transport chain. *Cell*. Vol.117, No.6, pp.773-786.

Rossano, F.; Ortega de Luna, L.; Buommino, E.; Cusumano, V.; Losi, E. & Catania, M.R. (1999). Secondary metabolites of Aspergillus exert immunobiological effects on human monocytes. *Res. Microbiol*. Vol.150, No.1, pp.13–19.

Rotig, A.; Cormier, V.; Blanche, S.; Bonnefont, J.P.; Ledeist, F.; Romero, N.; Schmitz, J.; Rustin, P.; Fischer, A. & Saudubray, J.M. (1990). Pearson's marrow-pancreas syndrome. A multisystem mitochondrial disorder in infancy. *J. Clin. Invest*. Vol.86, No.5, pp.1601-1608.

Rustin, P.; Chretien, D.; Bourgeron, T.; Gerard, B.; Rotig, A.; Saudubrary, J.M. & Munnich, A. (1994). Biochemical and molecular investigations in respiratory chain deficiencies. *Clin. Chim. Acta*. Vol.228, No.1, pp.35-51.

Sass, G.; Heinlein, S.; Agli, A.; Bang, R.; Schumann, J. & Tiegs, G. (2002). Cytokine expression in three mouse models of experimental hepatitis. *Cytokine*. Vol.19, No.3, pp.115-20.

Savel, H.; Forsyth, B.; Schaeffer, W. & Cardella, T. (1970). Effect of aflatoxin B1 upon phytohemagglutinin-transformed human lymphocytes. *Proc. Soc. Exp. Biol. Med*. Vol.134, No.4, pp.1112–1115.

Shaban, S.; Marzouqi, F.; Al Mansouri, A.; Penefsky, HS. & Souid, A-K. (2010). Oxygen measurements via phosphorescence. *Computer Methods and Programs in Biomedicine*. Vol.100, No.3, pp.265-268.

Slee, E.A.; Zhu, H.; Chow, S.C.; MacFarlane, M.; Nicholson, D.W. & Cohen, G.M. (1996). Benzylooxycarbonyl-Val-Ala-Asp (Ome) fluormethylketone (Z-VAD.FMK) inhibits apoptosis by blocking the processing of CPP32. *Biochemistry Journal*. Vol.315, No. (Pt 1), pp.21-24.

Souid, A-K.; Tacka, KA.; Galvan, KA. & Penefsky, HS. (2003). Immediate effects of anticancer drugs on mitochondrial oxygen consumption. *Biochemical Pharmacology*. Vol.66, No.6, pp.977-987.

Souid, A-K.; Penefsky, H.S..; Sadowitz, P.D. & Toms, B. (2006). Enhanced cellular respiration in cells exposed to doxorubicin. *Molecular Pharmaceutics*. Vol.3, No.3, pp.307-321.

Stec, J., Zmudzki, J., Rachubik, J., & Szczotka, M. (2009). Effects of aflatoxin B1, ochratoxin A, Patulin, citrinin, and zearalenone on the in vitro proliferation of pig blood lymphocytes. *Bull. Vet. Inst. Pulawy*. Vol53, No.1, pp129-134.

Sun, X.M.; Zhang, X.H.; Wang, H.Y.; Cao, W.J.; Yan, X.; Zuo, L.F.; Wang, J.L. & Wang, F.R. (2002). Effects of sterigmatocystin, deoxynivalenol and afaltoxin G1 on apoptosis of human blood lymphocytes in vitro. *Biomed. Environ. Sci*. Vol.15, No.2, pp.145-152.

Tacka, KA.; Dabrowiak, JC.; Goodisman, J.; Penefsky, HS. & Souid, A-K. (2004a). Quantitative studies on cisplatin-induced cell death. *Chemical Research in Toxicology*. Vol.17, No.8, pp.1102-1111.

Tacka, K.A..; Szalda, D.; Souid, A.-K..; Goodisman, J. & Dabrowiak, J.C. (2004b). Experimental and theoretical studies on the pharmacodynamics of cisplatin in Jurkat cells. *Chemical Research in Toxicology*. Vol.17, No.11, pp.1434-1444.

Takeda, K.; Hayakawa, Y.; Van Kaer, L.; Matsuda, H.; Yaqita, H. & Okumura, K. (2000). Critical contribution of liver natural killer T cells to a murine model of hepatitis. *Proc Natl Acad Sci USA*. Vol..97, No.10, pp.5498-5503.

Tao, Z.; Withers, HG.; Penefsky, HS.; Goodisman, J. & Souid, A-K. (2006a). Inhibition of cellular respiration by doxorubicin. *Chemical Research in Toxicology*. Vol.19, No.8, pp.1051-1058.

Tao, Z.; Ahmad, SS.; Penefsky, HS.; Goodisman, J. & Souid, A-K. (2006b). Dactinomycin impairs cellular respiration and reduces accompanying ATP formation. *Molecular Pharmaceutics*. Vol.3, No.6, pp.762-772.

Tao, Z.; Goodisman, J.; Penefsky, HS. & Souid, A-K. (2007). Caspase activation by cytotoxic drugs (the caspase storm). *Molecular Pharmaceutics*. Vol.4, No.4, (Epub 2007 Apr 17), pp.583-595.

Tao, Z.; Jones, E.; Goodisman, J. & Souid, A-K. (2008a). Quantitative measure of cytotoxicity of anticancer drugs and other agents. *Analytical Biochemistry*. Vol.381, No.1, (Epub 2008 Jun 18), pp.43-52.

Tao, Z.; Goodisman, J. & Souid, A-K. (2008b). Oxygen measurement via phosphorescence: reaction of sodium dithionite with dissolved oxygen. *The Journal of Physical Chemistry A*. Vol.112, No.7, (Epub 2008 Jan 30), pp.1511-1518.

Tao, Z.; Morrow, MP.; Asefa, T.; Sharma, KK.; Duncan, C.; Anan, A.; Penefsky, HS.; Goodisman, J. & Souid, A-K. (2008c). Mesoporous silica nanoparticles inhibit cellular respiration. *Nano Letter*. Vol.8, No.5, (Epub 2008 Apr 1), pp.1517-1526.

Tao, Z.; Raffel, RA.; Souid, A-K. & Goodisman, J. (2009). Kinetic studies on enzyme-catalyzed reactions: oxidation of glucose, decomposition of hydrogen peroxide and their combination. *Biophysical Journal*. Vol.96, No.7, pp.2977-2988.

Tiegs, G.; Hentschel, J. & Wendel, A. (1992). A T-cell-dependent experimental liver injury in mice inducible by concanavalin A. *Journal Clinical Investigation*. Vol.90, No.1, pp.196-203.

Tiegs G. (1997). Experimental hepatitis and the role of cytokines. *Acta Gastroenterol Belg*. Vol.60, No.2, pp.176-9.

Universal library for measurements computing devices. http://www.mccdaq.com/daq-software/universal-library.aspx. Access May 2009.

Wang, L-Y.; Hatch, M.; Chen, C-J.; Levin, B.; You, S-L.; Lu, S-N.; Wu, M-H.; Wu, W-P.; Wang, L-W.; Wang, Q.; Huang, G-T.; Yang, P-M.; Lee, H-S. & Santella, R.M. (1996).

Aflatoxin exposure and risk of hepatocellular carcinoma in Taiwan. *International Journal Cancer*. Vol.67, No.5, pp.620-625.

Weiss, R.F. (1970). The solubility of nitrogen, oxygen, and argon in water and seawater. *Deep-Sea Research*. Vol.17, No.4, pp.721-735.

Whyte, DA.; Al-Hammadi, S.; Balhaj, G.; Brown, OM.; Penefsky, HS. & Souid, A-K. (2010). Cannabinoids inhibit cellular respiration of human oral cancer cells. *Pharmacology*. Vol.85, No.6, (Epub 2010 Jun 2), pp.328-335.

Williams, J.H.; Phillips, T.D.; Jolly, P.E.; Stiles, J.K.; Jolly, C.M. & Aggarwal, D. (2004). Human aflatoxicosis in developing countries: a review of toxicology, exposure, potential health consequences, and interventions. *American Journal of Clinical Nutrition*. Vol.80, No.5, pp.1106-1122.

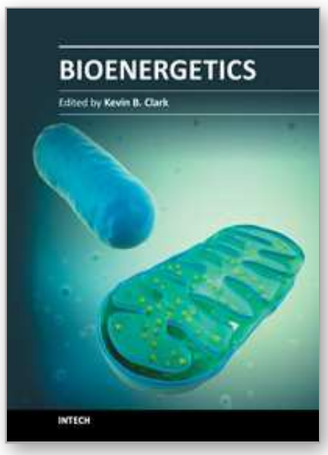

Bioenergetics

Edited by Dr Kevin Clark

ISBN 978-953-51-0090-4
Hard cover, 272 pages
Publisher InTech
Published online 02, March, 2012
Published in print edition March, 2012

Cellular life depends upon energy storage, transformation, utilization, and exchange in order to optimally function and to stay-off death. The over 200-year-old study of how cells transform biological fuels into usable energy, a process broadly known as bioenergetics, has produced celebrated traditions in explaining origins of life, metabolism, ecological adaptation, homeostasis, biosynthesis, aging, disease, and numerous other life processes. InTech's edited volume, Bioenergetics, brings together some of these traditions for readers through a collection of chapters written by international authorities. Novice and expert will find this book bridges scientific revolutions in organismic biology, membrane physiology, and molecular biology to advance the discipline of bioenergetics toward solving contemporary and future problems in metabolic diseases, life transitions and longevity, and performance optimization.

INTECH
open science | open minds

InTech Europe
University Campus STeP Ri
Slavka Krautzeka 83/A
51000 Rijeka, Croatia
Phone: +385 (51) 770 447
Fax: +385 (51) 686 166
www.intechopen.com

InTech China
Unit 405, Office Block, Hotel Equatorial Shanghai
No.65, Yan An Road (West), Shanghai, 200040, China
中国上海市延安西路65号上海国际贵都大饭店办公楼405单元
Phone: +86-21-62489820
Fax: +86-21-62489821

IntechOpen